JACS
JOURNAL OF THE AMERICAN CHEMICAL SOCIETY

ARTICLE

pubs.acs.org/JACS

Supramolecular Strategies To Construct Biocompatible and Photoswitchable Fluorescent Assemblies

Ibrahim Yildiz,[†] Stefania Impellizzeri,[†] Erhan Deniz,[†] Bridgeen McCaughan,[‡] John F. Callan,*[,‡] and Françisco M. Raymo*[,†]

[†]Department of Chemistry, University of Miami, 1301 Memorial Drive, Coral Gables, Florida 33146-0431, United States

[‡]Department of Pharmacy and Pharmaceutical Sciences, School of Biomedical Sciences, University of Ulster, Coleraine BT52 1SA, Northern Ireland, United Kingdom

Supporting Information

ABSTRACT: We designed and synthesized an amphiphilic copolymer with pendant hydrophobic decyl and hydrophilic poly(ethylene glycol) chains along a common poly(methacrylate) backbone. This macromolecular construct captures hydrophobic boron dipyrromethene fluorophores and hydrophobic spiropyran photochromes and transfers mixtures of both components in aqueous environments. Within the resulting hydrophilic supramolecular assemblies, the spiropyran components retain their photochemical properties and switch reversibly to the corresponding merocyanine isomers upon ultraviolet illumination. Their photoinduced transformations activate intermolecular electron and energy transfer pathways, which culminate in the quenching of the boron dipyrromethene fluorescence. As a result, the emission intensity of these supramolecular constructs can be modulated in aqueous environments under optical control. Furthermore, the macromolecular envelope around the fluorescent and photochromic components can cross the membrane of Chinese hamster ovarian cells and transport its cargo unaffected into the cytosol. Indeed, the fluorescence of these supramolecular constructs can be modulated also intracellularly by operating the photochromic component with optical inputs. In addition, cytotoxicity tests demonstrate that these supramolecular assemblies and the illumination conditions required for their operation have essentially no influence on cell viability. Thus, supramolecular events can be invoked to construct fluorescent and photoswitchable systems from separate components, while imposing aqueous solubility and biocompatibility on the resulting assemblies. In principle, this simple protocol can evolve into a general strategy to deliver and operate intracellularly functional molecular components under optical control.

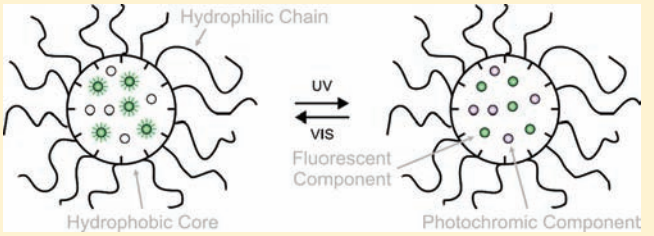

INTRODUCTION

Photochromic molecules interconvert reversibly between states with a distinct absorption signature across the ultraviolet and visible regions of the electromagnetic spectrum.[1−6] In most instances, the interconvertible states also differ significantly in their stereoelectronic properties. In fact, the structural and electronic changes, accompanying their photoinduced and reversible transformations, can be engineered to control the emission of complementary fluorophores.[6−8] Specifically, fluorescent and photochromic components can be integrated within a common covalent skeleton, and the emission of the former can be modulated by interconverting the latter under optical control. Accordingly, numerous examples of fluorophore−photochrome dyads have already been developed,[9−13] and their operating principles for fluorescence modulation have recently been extended to nanostructured constructs[14−18] and extensively reviewed.[8] In most instances, electron and energy transfer processes dominate the excited-state dynamics of these multicomponent assemblies and dictate their emission signature. In particular, the transfer of one electron from/to the excited state of the fluorophore to/from only one of the two states of the photochrome or the transfer of energy from the excited fluorophore to only one of the two states of the photochrome is generally responsible for fluorescence modulation. The assembly of these fluorophore−photochrome constructs, however, often requires tedious multistep procedures, which considerably limit their synthetic accessibility. In addition, most of these functional compounds are rather hydrophobic and can only be operated in organic solvents. In fact, it is not entirely clear whether their photochemical and photophysical properties would at all survive the transition from organic to aqueous environments necessary for the application of these fluorescent photoswitches in biomedical research. Indeed, it is becoming apparent that the ability of a photochromic element to switch fluorescence, in combination with appropriate illumination protocols, can offer the opportunity to overcome diffraction and permit the visualization of biological samples with resolution at the nanometer level.[19] In fact, fluorophore−photochrome

Received: August 20, 2010
Published: December 23, 2010

dx.doi.org/10.1021/ja107341f | J. Am. Chem. Soc. 2011, 133, 871–879

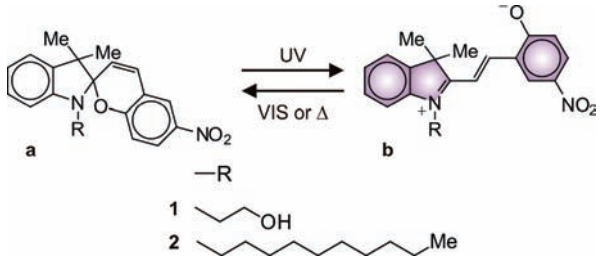

Figure 1. Photoinduced and reversible transformation of the spiropyrans **1a** and **2a** into the merocyanines **1b** and **2b**.

constructs can become, in principle at least, invaluable analytical tools for the super-resolution imaging of cells and tissues.[20−32] However, it is first necessary to identify viable strategies to impose biocompatibility on them, without complicating their synthesis even further, and to operate effectively these functional assemblies in water.

Recently, we designed and investigated a photoswitchable fluorescent dyad consisting of a boron dipyrromethene (BODIPY) fluorophore covalently connected to a spiropyran photochrome.[13a] In acetonitrile, the ultraviolet illumination of this compound promotes the conversion of the spiropyran component into the corresponding merocyanine. This photoinduced transformation facilitates the transfer of one electron or energy from the BODIPY to the merocyanine component upon visible excitation of the former with concomitant fluorescence quenching. The photogenerated and nonfluorescent state reverts thermally to the original fluorescent species and restores the initial emission intensity. As a result, the fluorescence of this fluorophore−photochrome dyad can be switched off and on for multiple cycles simply by turning on and off, respectively, an ultraviolet source, while illuminating the sample with visible radiations. To impose hydrophilic character on this hydrophobic construct, we appended covalently multiple copies of this dyad to a common hydrophilic polymer backbone. The fluorescence of the resulting macromolecular system could be modulated in water under optical control, but only with slow switching speeds and poor fatigue resistance. In addition, this hydrophilic assembly of fluorescent and photochromic components required multiple and tedious synthetic steps for its preparation. In search of strategies to overcome these limitations, we envisaged the possibility of invoking supramolecular events to assemble biocompatible fluorescent switches with good photochemical performance in water. Specifically, we relied on the established ability of amphiphilic building blocks to form hydrophilic micellar aggregates capable of encapsulating hydrophobic guests[33−37] to construct functional supramolecular assemblies of simple and separate fluorescent and photochromic components. In this paper, we report the preparation of these systems as well as the characterization of their spectroscopic properties, the investigation of their ability to cross cell membranes, and the assessment of their cytotoxicty.

RESULTS AND DISCUSSION

Design, Synthesis, and Spectroscopy. The spiropyran **1a** (Figure 1) switches to the merocyanine **1b** upon ultraviolet illumination in acetonitrile.[38] This photoinduced transformation shifts the reduction potential in the negative direction by 0.3 V and turns the transfer of one electron from the excited BODIPY **3** (Figure 2) to the photochromic compound from endergonic to

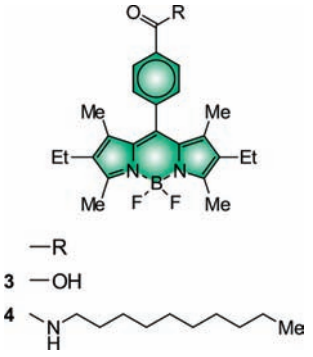

Figure 2. Structures of the BODIPY derivatives **3** and **4**.

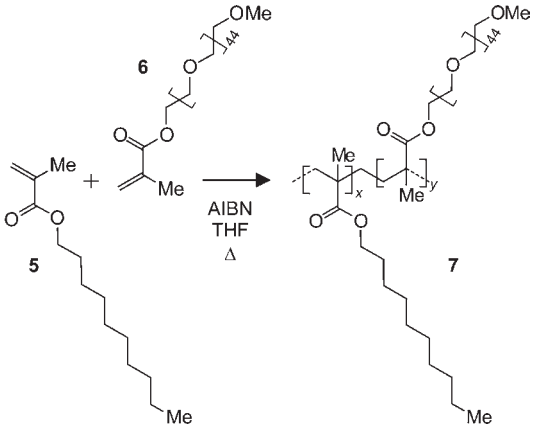

Figure 3. Polymerization of the monomers **5** and **6** to generate the copolymer **7**.

exergonic with an estimated free energy change of ca. −0.2 eV.[13a] In addition, the formation of **1b** results in the appearance of an intense absorption band in the same region of wavelengths where **3** emits.[13a] The significant overlap between the absorption of one and the emission of the other can promote the transfer of energy from the excited fluorophore to the photogenerated state of the photochrome. Thus, both electron and energy transfer processes can contribute to quench the emission of the fluorophore with the photochromic transformation. Fluorescent and photochromic components, however, must be in close proximity for the electron or energy transfer process to occur. In addition, the modulation of fluorescence in biological media requires aqueous compatibility, and **1a** is not soluble in water. On the basis of these considerations, we designed an amphiphilic polymer expected to encapsulate both the fluorescent and photochromic components in its interior and enforce a close separation between them, while ensuring aqueous solubility of the overall supramolecular assembly. In particular, we synthesized the methacrylate monomers **5** and **6** (Figure 3) with hydrophobic decyl and hydrophilic poly(ethylene glycol) chains, respectively, and reacted them, under the assistance of azobisisobutyronitrile (AIBN), to generate the amphiphilic copolymer **7**.[39] The ^{1}H nuclear magnetic resonance (NMR) spectrum of the resulting macromolecular construct reveals the ratio between the hydrophobic and hydrophilic chains appended to the main polymer backbone to be ca. 2.3. Gel permeation chromatography (GPC) indicates this particular copolymer to have a number average molecular weight (M_n) of 46 800 with a polydispersity index (PDI) of 1.73. Its hydrophilic poly(ethylene glycol) chains ensure solubility in water, and its

dx.doi.org/10.1021/ja107341f |J. Am. Chem. Soc. 2011, 133, 871–879

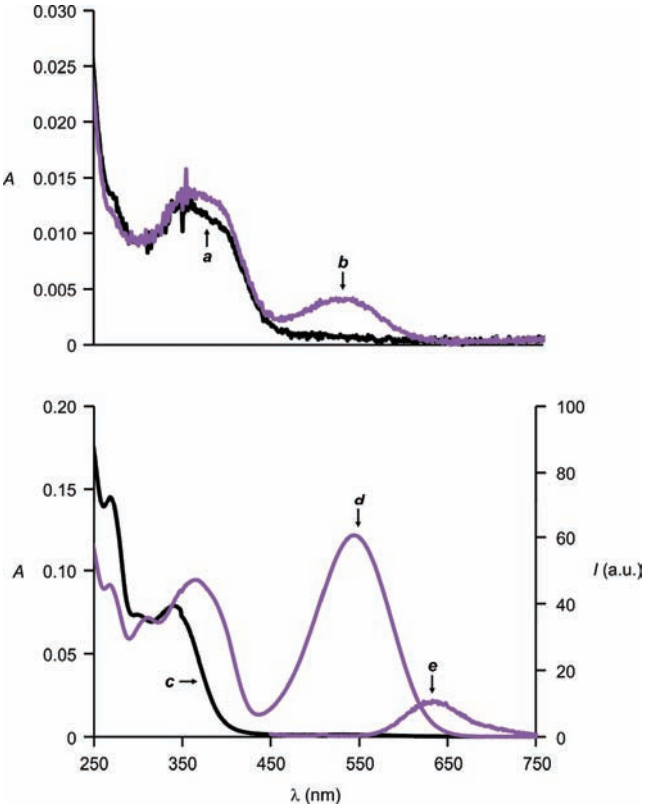

Figure 4. Absorption spectra of PBS dispersions (pH 7.4, 20 °C) of polymer micelles containing **1a** (curves a and b) or **2a** (curves c and d) recorded after equilibration in the dark for 12 h before (curves a and c) and after (curves b and d) irradiation (365 nm, 0.4 mW cm^{-2}, 5 min). Emission spectrum (curve e, λ_{ex} = 434 nm) of a PBS dispersion of polymer micelles containing **2a** after equilibration and irradiation.

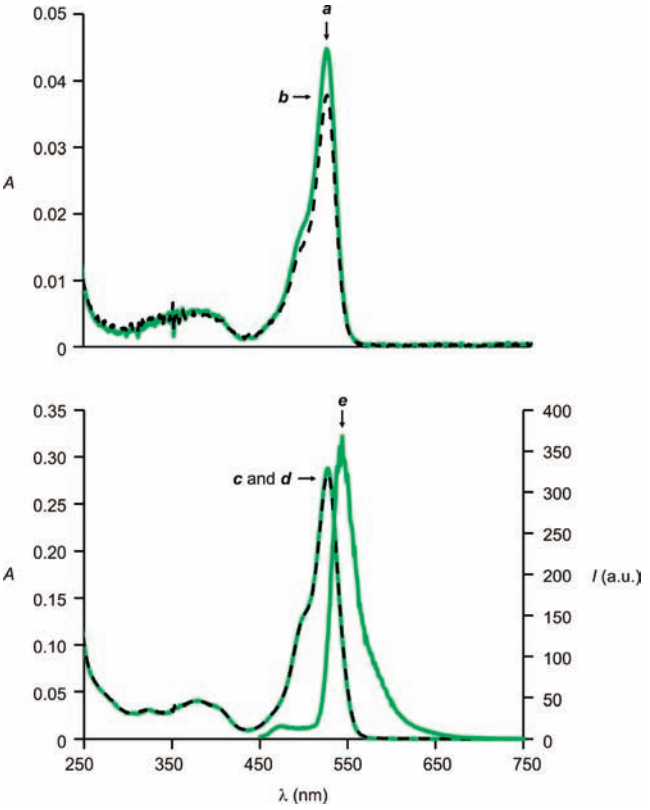

Figure 5. Absorption spectra of PBS dispersions (pH 7.4, 20 °C) of polymer micelles containing **3** before (curve a) and after (curve b) irradiation (365 nm, 0.4 mW cm^{-2}, 5 min) or **4** before (curve c) and after (curve d) irradiation. Emission spectrum (curve e, λ_{ex} = 434 nm) of a PBS dispersion of polymer micelles containing **4**.

hydrophobic decyl chains encourage the formation of supramolecular aggregates with an average hydrodynamic diameter of 18 nm, according to dynamic light scattering (DLS) measurements. The comparison of this value to the hydrodynamic diameters of polystyrene standards of known molecular weight[40] suggests that an average of four amphiphilic copolymer units assemble into a single micellar construct. Similarly, transmission electron microscopy (TEM) images (Figure S1a, Supporting Information) of the resulting assemblies show globular particles with an average diameter of 17 nm.

The spiropyran **1a** is essentially insoluble in water at ambient temperature, but dissolves in phosphate-buffered saline (PBS) with a pH of 7.4 in the presence of **7**. Indeed, the corresponding absorption spectrum (curve a in Figure 4) reveals the characteristic band of **1a** at 340 nm. The low absorbance of this band, however, indicates that **7** can transfer only micromolar amounts of **1a** in aqueous environments. Nonetheless, the photochromic components entrapped within the polymer micelles retain their photochemical character, and the band of **1b** appears at 538 nm upon ultraviolet irradiation (curve b in Figure 4).

The BODIPY **3** is also sparingly soluble in water, but readily dissolves in PBS in the presence of **7**. Consistently, the absorption spectrum (curve a in Figure 5) of a PBS dispersion of **3** and **7** shows the characteristic band of the BODIPY fluorophore at 522 nm. Upon ultraviolet irradiation under conditions normally required to operate spiropyrans, however, the absorbance of **3** decreases significantly (curve b in Figure 5). This trend is indicative of the photoinduced degradation of the fluorophore and suggests that, despite interactions with the amphiphilic polymer, **3** is exposed to water (vide infra).

To facilitate the entrapment of guests within **7** and prevent their exposure to water, we designed and synthesized the spiropyran **2a** (Figures 1 and S2, Supporting Information) and the BODIPY **4** (Figure 2). Both compounds bear a hydrophobic decyl chain, which is expected to bury the photochromic and fluorescent components further into the hydrophobic interior of the supramolecular construct. Indeed, the absorption spectrum (curve c in Figure 4) of a PBS dispersion of **2a** and **7** reveals an intense absorption at 340 nm for the spiropyran guests trapped within the micellar hosts. In addition, a band for **2b** appears at 544 nm after ultraviolet irradiation (curve d in Figure 4), while that of **1b** is positioned at 538 nm under otherwise identical conditions. The elongation in wavelength demonstrates that the environment around **2b** is more hydrophobic than that surrounding **1b**. In fact, the absorption wavelength of merocyanines is known to increase with a decrease in solvent polarity.[41] Furthermore, the spectroscopic signature of **2a** and **2b** within the polymer micelles resembles that recorded in acetonitrile (curves a and b in Figure S3, Supporting Information). In both instances, the ratio between the two isomers is ca. 70:30 at the photostationary state, albeit the absorption band of the photogenerated species is positioned at 562 nm in acetonitrile.

The merocyanine **2b** reverts spontaneously back to **2a** within the polymer micelles, and concomitantly, the absorbance at 544 nm

dx.doi.org/10.1021/ja107341f | J. Am. Chem. Soc. 2011, 133, 871–879

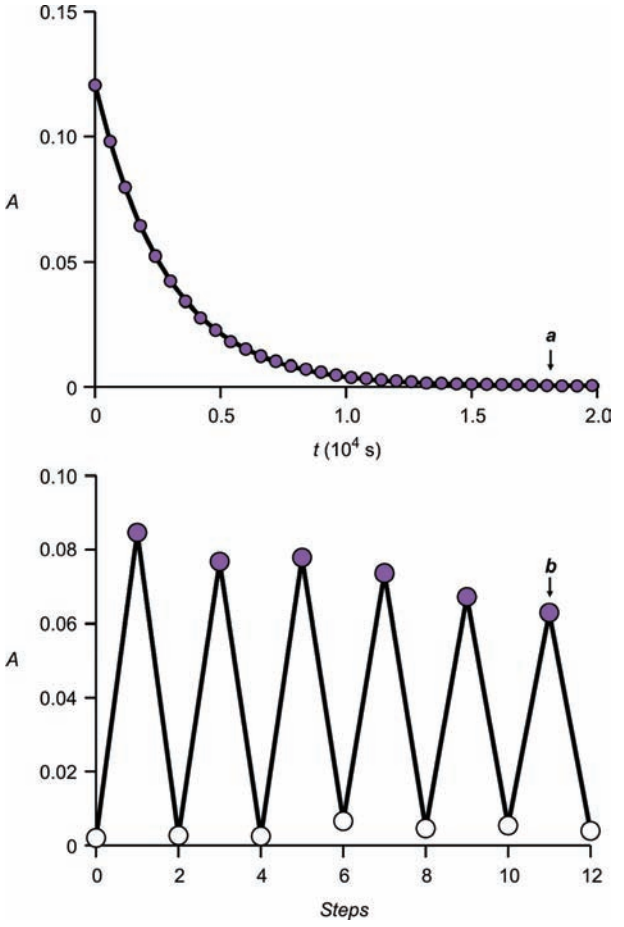

Figure 6. Absorbance evolution at 545 nm of a PBS dispersion (pH 7.4, 20 °C) of polymer micelles containing **2a** recorded after equilibration in the dark for 12 h and either with ultraviolet irradiation (curve a, 365 nm, 0.4 mW cm^{-2}, 5 min) or with alternating irradiation steps (curve b) at ultraviolet and visible (562 nm, 0.3 mW cm^{-2}, 5 min) wavelengths.

(curve a in Figure 6) decays over the course of several minutes. Curve fitting of the corresponding absorbance profile indicates the reisomerization rate constant to be 4×10^{-4} s^{-1}. This value is approximately 1 order of magnitude smaller than that (cf. 2×10^{-3} s^{-1}) measured in acetonitrile (curve c in Figure S3, Supporting Information) and comparable to that determined for similar merocyanines in dimethylformamide,[41] suggesting, once again, the presence of a relatively hydrophobic environment around the photochromic switch within the polymer micelles. Similarly, **2b** also reverts back to **2a** upon visible illumination, and in fact, the photochromic compounds entrapped within the polymeric assembly can be switched back and forth between their two states by alternating ultraviolet and visible irradiation steps (curve b in Figure 6).

In analogy to the photochrome **2a**, the fluorophore **4** also tends to localize within the hydrophobic interior of the polymeric assembly. The corresponding absorption spectrum (curve c in Figure 5) shows the BODIPY absorption at 528 nm and does not change after ultraviolet illumination (curve d in Figure 5), indicating that the macromolecular envelope protects the fluorophore from the aqueous environment. Indeed, control experiments in the absence of the polymer host demonstrate that the exposure of **4** to water encourages photobleaching. Specifically, the absorption spectrum of **4** in acetonitrile shows the BODIPY absorption at 523 nm and, once again, does not change with ultraviolet irradiation (curves a and b in Figure S4, Supporting Information). Instead, the BODIPY absorbance decreases significantly in a mixture of acetonitrile and water (2:1, v/v) under identical irradiation conditions (curves c and d in Figure S4). Thus, the amphiphilic copolymer **7** is particularly effective in maintaining either **2a** or **4** within a relatively hydrophobic environment and limiting their exposure to water. On the contrary, conventional phospholipid micelles cannot ensure the same level of protection to their hydrophobic guests, at least in the case of **4**. Indeed, the absorption spectra (Figure S5, Supporting Information) of **4**, entrapped within micelles prepared from the ammonium salt of 1,2-dipalmitoyl-*sn*-glycero-3-phosphoethanolamine *N*-(methoxy(polyethylene glycol)-2000),[42] reveal a significant decrease in absorbance with ultraviolet irradiation. Nonetheless, the behavior of **2a** under these conditions (Figure S6, Supporting Information) is similar to that observed in the presence of **7**. In both instances, **2a** switches to **2b** under ultraviolet irradiation with the appearance of a band essentially at the same wavelength and the photogenerated isomer reverts back to the original one with similar kinetics.

The emission spectrum (curve e in Figure 5) of a PBS dispersion of **4** and **7** shows the characteristic BODIPY fluorescence at 544 nm with a quantum yield of 0.44. In acetonitrile, the emission of **4** is centered at a similar wavelength (cf. 539 nm), but the quantum yield is 0.81. The depressive effect of the polymer micelles on the fluorescence quantum yield is, presumably, a result of their ability to bring multiple dyes in close proximity within their hydrophobic interior and encourage self-quenching. In any case, the emission band of **4** within the supramolecular constructs is in the same region of wavelengths where **2b** absorbs under the same experimental conditions. Thus, the entrapment of **4** and **2b** within the same macromolecular host is expected to result in the transfer of energy from the former to the latter upon excitation. In addition, electron transfer from the excited BODIPY to the photogenerated isomer of the photochromic system is exergonic[13a] and, if the two components are sufficiently close within their supramolecular container, can also occur as an alternative to energy transfer. It follows that the photoinduced and reversible interconversion of **2a** and **2b** within a polymer micelle also containing **4** is expected to modulate the emission intensity of the BODIPY fluorophores. Indeed, the absorption and emission spectra (curves a and c in Figure 7) of a PBS dispersion of **2a**, **4**, and **7** show the typical absorbance and fluorescence of the BODIPY components at 528 and 542 nm, respectively. Upon ultraviolet irradiation, **2a** switches to **2b**, and the absorption band of the merocyanine isomer appears in the corresponding spectrum (curve b in Figure 7). The absorbance of this band indicates the ratio between **2a** and **2b** to be, once again, ca. 70:30 at the photostationary state. This transformation activates the expected electron and energy transfer pathways and causes a significant decrease in the emission intensity at 542 nm (curve d in Figure 7) with a quenching efficiency of 0.8. Concomitantly, the characteristic fluorescence of the photogenerated merocyanines[38] develops at 638 nm. Indeed, this additional band resembles that observed for **2b** (curve e in Figure 4) within the polymer micelles in the absence of **4**, under otherwise identical conditions. Nonetheless, the presence of **4** translates into a significant enhancement in the fluorescence of **2b**. In fact, a comparison of the integrated emission intensities, recorded with and without **4**, suggests that the fractional contribution of direct excitation to the total emission intensity of **2b** is only 0.3 and that

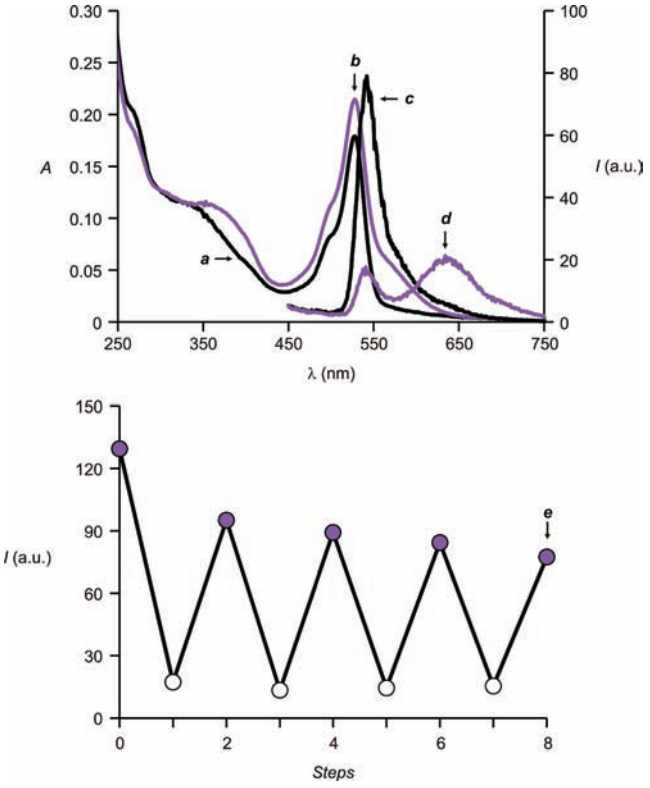

Figure 7. Absorption spectra of a PBS dispersion (pH 7.4, 20 °C) of polymer micelles containing **2a** and **4** recorded after equilibration in the dark for 12 h before (curve a) and after (curve b) irradiation (365 nm, 0.4 mW cm^{-2}, 5 min). Emission spectra (λ_{ex} = 434 nm) of the same dispersion after equilibration and before (curve c) and after (curve d) irradiation. Evolution of the emission intensity at 545 nm of the same dispersion after equilibration and with alternating irradiation steps (curve e) at ultraviolet and visible (562 nm, 0.3 mW cm^{-2}, 5 min) wavelengths.

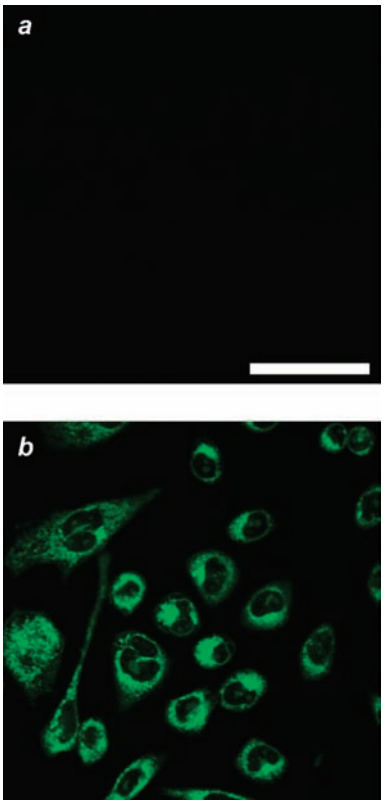

Figure 8. Confocal fluorescence images (λ_{ex} = 514 nm, λ_{em} = 535−635 nm, scale bar = 50 μm) of CHO cells recorded before (a) and after (b) incubation with a PBS dispersion (10%, v/v) of **2a**, **4**, and **7** for 24 h.

the expected transfer of energy from the excited BODIPY components to the photogenerated isomers of the photochromic switches is predominantly responsible for the detected merocyanine fluorescence. Thus, these observations demonstrate that the copolymer **7** is able to wrap around the fluorescent and photochromic components and maintain them in sufficiently close proximity to permit fluorescent modulation. Interestingly, DLS measurements reveal that the hydrodynamic diameter of the polymer micelles grows from 18 nm (vide supra) to 37 nm in the presence of **2a** and **4** with an increase of the average number of polymer chains per micelle from 4 to 19. Consistently, TEM images (Figure S1b, Supporting Information) also show an increase in the average diameter of the polymer micelles from 17 nm (vide supra) to 35 nm in the presence **2a** and **4**. Thus, the hydrophobic guests affect the ability of the macromolecular host to assemble into supramolecular constructs and control the physical dimensions of the resulting aggregates.

As observed in the absence of **4**, **2b** spontaneously reverts back to **2a** with first-order kinetics on a time scale of minutes. As a result, its absorbance in the visible region decays (Figure S7, Supporting Information) and the initial emission intensity of **4** is restored. Similarly, the photogenerated species **2b** switches back to **2a** also under visible irradiation, and in fact, the emission intensity of its fluorescent partner **4** can be modulated for multiple switching cycles by alternating ultraviolet and visible irradiation steps (curve e in Figure 7). Interestingly, a plot of the absorbance of **2b** against the number of switching steps is essentially identical to that recorded in the absence of the BODIPY component (curve b in Figure 6) and shows a decrease of ca. 8% after four switching cycles. Instead, the emission intensity of the BODIPY component drops by ca. 40% after the same number of switching cycles. This behavior suggests that the fluorescent component is more susceptible to photodegradation than the photochromic one under these experimental conditions.

Intracellular Fluorescence Modulation and Cytotoxicity Assays. The ability of the amphiphilic copolymer **7** to transport **2a** and **4** across cell membranes was assessed by confocal microscopy using Chinese hamster ovarian (CHO) cells. Indeed, polymers with pendant poly(ethylene glycol) chains are known to enter cells and transport intracellularly even relatively large inorganic nanoparticles.[43,44] Although the exact mechanism responsible for intracellular accumulation is not clear at this stage, endocytosis has previously been shown to result in the localization of similarly sized nanostructured assemblies in endosomes.[43] In our experiments, CHO cells were imaged before and after (parts a and b, respectively, of Figure 8) incubation with a PBS dispersion of **2a**, **4**, and **7** for 24 h. The resulting images reveal fluorescence within the cells only after their incubation with the polymer micelles. In particular, the fluorescent supramolecular assemblies cross the cell membrane and accumulate preferentially in the cytosol with limited localization in the nucleus. Furthermore, the punctuate intracellular distribution of the fluorescent constructs suggests their accumulation in restricted cytosolic compartments, such as endosomes/vesicles. In addition, a stack of images (Figure S8, Supporting Information), recorded along

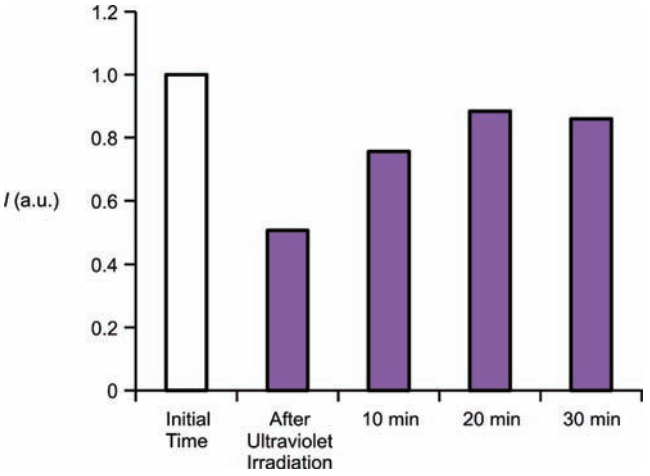

Figure 9. Emission intensity of CHO cells measured with a plate reader (λ_{ex} = 434 nm, λ_{em} = 550 nm) after incubation with a PBS dispersion (10%, v/v) of **2a**, **4**, and **7** for 24 h before irradiation, immediately after irradiation (365 nm, 0.4 mW cm^{-2}, 1 min), and 10, 20, and 30 min after irradiation, reported relative to that determined for identical cells incubated without **2a** under otherwise identical conditions.

the optic axis, reveals consistent fluorescence evolution in the vertical direction, indicating that the fluorophores remain trapped inside the polymer micelles, rather than associating with the cell membrane.

The profile of the emission intensity measured along lines drawn across cells (curves a−f in Figure S9, Supporting Information) incubated with a PBS dispersion of **2a**, **4**, and **7** for 24 h shows the predominant localization of the fluorescent constructs at the periphery of the cells, rather than in their central region. Upon ultraviolet illumination, **2a** switches to **2b** and the fluorescence of **4** decreases (curves g−l in Figure S9). A similar analysis for cells incubated only with **4** and **7**, under otherwise identical conditions, shows instead negligible changes in fluorescence with ultraviolet irradiation (Figure S10, Supporting Information). In fact, a comparison of the average emission intensity, integrated along the drawn lines, shows a decrease of ca. 33% upon ultraviolet irradiation only in the presence of **2a** within the polymer micelles (Figure S11, Supporting Information). Thus, the ability of the photochromic component to switch the emission of its fluorescent partner under optical control, observed in aqueous solutions (vide supra), can be reproduced even within living cells. These observations indicate that the copolymer **7** can transport the fluorescent and photochromic components **2a** and **4** inside cells and maintain them in close proximity within the intracellular environment to permit fluorescence modulation.

To further support the ability of the photochromic component to modulate the emission of its fluorescent partner intracellularly, the fluorescence of CHO cells (Figure 9), incubated with a PBS dispersion of **2a**, **4**, and **7** in a well plate for 24 h, was measured with a plate reader relative to that of identical cells incubated without **2a**, under otherwise identical conditions. After ultraviolet irradiation for only 30 s, the detected emission intensity decreases to ca. 40% of the original value (Figure 9), in agreement with the expected photoinduced interconversion of **2a** into **2b** with concomitant suppression of the fluorescence of **4**. Upon storage of the sample in ambient light, the photogenerated state **2b** of the photochromic system gradually reverts back to the original isomer **2a**, and the fluorescence of **4** is restored over the course of several minutes. On the contrary, the fluorescence of cells incubated with a PBS dispersion of only **4** and **7**, under otherwise identical conditions, does not change significantly with ultraviolet illumination. Thus, the presence of the photochromic component within the cells is essential to switch fluorescence with optical inputs.

The cytotoxicity of the polymer micelles, containing **2a** and **4**, as well as of the irradiation conditions required to switch intracellularly the photochromic component was assessed with the Trypan Blue assay.[45] This particular organic dye stains exclusively dead/dying cells and offers the opportunity to determine the fraction of living cells (viability). Specifically, the viability was determined for cells either incubated with increasing amounts (0−25%, v/v) of a PBS dispersion of **2a**, **4**, and **7** (Figure S12a, Supporting Information) or illuminated for increasing irradiation times (0−1200 s) at ultraviolet wavelengths (Figure S12b). In both instances, the cell viability remains essentially unchanged. Thus, both the polymer micelles and the illumination conditions required for their operations do not have any significant toxicity on the CHO cells.

CONCLUSIONS

An amphiphilic copolymer with hydrophobic decyl chains and hydrophilic poly(ethylene glycol) tails along a common poly(methacrylate) backbone captures mixtures of BODIPY fluorophores and spiropyran photochromes and transfers them in aqueous phase. Hydrophobic decyl tails, however, must be attached to the fluorescent and photochromic guests to bury them within the hydrophobic interior of the macromolecular envelope to prevent their exposure to water and preserve their photochemical and photophysical properties. Within the resulting supramolecular constructs, the photoinduced and reversible transformation of the spiropyrans into the corresponding merocyanines activates electron and energy transfer pathways and quenches the BODIPY fluorescence. As a result, the emission intensity of these systems can be modulated under optical control by switching the photochromic components between their two states. Furthermore, the amphiphilic supramolecular container can cross cell membranes, transport its cargo into the cytosol, and permit the intracellular modulation of fluorescence. In addition, both the supramolecular systems and the irradiation conditions required for their operation are not cytotoxic. Thus, this simple supramolecular strategy to assemble photoswitchable fluorescent constructs from separate fluorophores and photochromes and impose biocompatibility on them can evolve into a valuable protocol for the intracellular delivery and operation of functional molecular components. In particular, the cellular internalization of photoswitchable fluorophores can offer the opportunity to visualize subcellular components with subdiffraction resolution under the influence of patterned or sequential multiphoton illumination. Hence, our protocol for the assembly of biocompatible fluorescent probes with photoswitchable character can have profound implications in super-resolution imaging and, ultimately, facilitate the experimental implementation of this collection of promising analytical techniques for the investigation of biological specimens at the nanoscale.

EXPERIMENTAL PROCEDURES

Materials and Methods. CH_2Cl_2 and MeCN were distilled over CaH_2. THF was distilled over Na/benzophenone. H_2O (18.2 MΩ cm) was purified with a Barnstead International NANOpure DIamond Analytical system. Methacrylic acid was vacuum distilled. AIBN was crystallized

twice from methanol. All other chemicals were used as received from commercial sources. Compounds **1a** and **3** were prepared following literature procedures.[13a,38] All reactions were monitored by thin-layer chromatography, using aluminum sheets coated with silica (60, F_{254}). Fast atom bombardment mass spectrometry (FABMS) spectra were recorded with a VG Mass Lab Trio-2 spectrometer in a 3-nitrobenzyl alcohol matrix. NMR spectra were recorded with Bruker Avance 300 and 400 spectrometers. GPC was performed with a Phenomenex Phenogel 5-μm MXM column (7.8 × 300 mm) operated with a Varian ProStar system, coupled to a ProStar 330 photodiode array detector, in THF at a flow rate of 1.0 mL min^{-1}. Monodisperse polystyrene standards (2700−200000) were employed to determine the M_n and PDI of the polymers from the GPC traces. DLS experiments were performed in quartz cells (3 × 3 mm) with a Coulter N4 Plus apparatus, operating at a wavelength of 632.8 nm (10 mW) with an orthogonal geometry. The samples were dissolved in H_2O (3 mL), filtered through Pall Corp. syringe filters (0.1 μm) five times, and stored. The concentration was adjusted to ensure scattering intensities in the range from 5×10^4 to 1×10^6 counts/s. The nanoparticle size was calculated by averaging the values of five runs of 300 s in unimodal size mode. TEM images were recorded with an FEI Tecnai 12 microscope on copper grids (200 mesh) using a uranyl acetate stain. Absorption spectra were recorded with a Varian Cary 100 Bio spectrometer, using quartz cells with a path length of 0.5 cm. Emission spectra were recorded with a Varian Cary Eclipse spectrometer in aerated solutions. Fluorescence quantum yields were determined with fluorescein and rhodamine B standards, according to a literature procedure.[46] The samples were irradiated at 365 nm (0.4 mW cm^{-2}) with a Mineralight UVGL-25 lamp and at 562 nm (0.3 mW cm^{-2}) with a Spectral Energy LH 150/1 light source. The output power at both wavelengths was determined with a Newport 1815-C power meter.

Synthesis of ***8***. A solution of 2,3,3-trimethylindolenine (1 g, 6 mmol) and 1-bromodecane (4.2 g, 19 mmol) in MeCN (15 mL) was heated under reflux and Ar for 12 h. After the solution was cooled to ambient temperature, the solvent was distilled off under reduced pressure. The residue was washed with Et_2O (3 × 30 mL) and dried under reduced pressure to afford **8** (1.2 g, 50%) as a red waxy solid. FABMS: m/z = 300 $[M - Br]^+$. ^1H NMR ($CDCl_3$): δ = 0.82 (3H, t, 13 Hz), 1.19−1.32 (12H, m), 1.41 (2H, m), 1.61 (6H, s), 1.89 (2H, t, 15 Hz), 2.87 (3H, s), 4.68 (2H, t, 15 Hz), 7.44−7.47 (1H, m), 7.51−7.54 (2H, m), 7.63 (1H, m). ^{13}C NMR ($CDCl_3$): δ = 14.4, 15.1, 22.9, 23.1, 23.5, 27.2, 28.4, 29.4, 29.5, 29.7, 32.2, 50, 54.5, 115.7, 123.1, 129.6, 130.4, 141.3, 142.1, 196.3.

Synthesis of ***2a***. A solution of 2-hydroxy-5-nitrobenzaldehyde (0.38 g, 2 mmol), **8** (0.86 g, 2 mmol), and piperidine (0.19 g, 2.3 mmol) in EtOH (10 mL) was heated under reflux for 3 h. The reaction mixture was allowed to cool to ambient temperature, and the solvent was distilled off under reduced pressure. The residue was purified by column chromatography [SiO_2:hexane/EtOAc (19:1, v/v)] to afford **2a** (0.35 g, 35%) as a light-orange solid. FABMS: m/z = 449 $[M + H]^+$. ^1H NMR ($CDCl_3$): δ = 0.89 (3H, t, 14 Hz), 1.14(3H, s), 1.19−1.34 (16H, m), 1.29 (3H, s), 3.14 (2H, m), 5.85 (1H, d, 8 Hz),6.58 (1H,d, 8 Hz), 6.75 (1H, d, 8 Hz), 6.89 (2H, m), 7.10 (1H, d, 8 Hz), 7.20 (1H, m), 8.01 (2H, m). ^{13}C NMR ($CDCl_3$): δ = 14.5, 20.3, 23.1, 26.4, 27.7, 29.4, 29.7, 29.8, 29.9, 30, 32.3, 44.2, 53.1, 107.2, 115.9, 118.9, 119.6, 122, 122.5, 123.1, 126.3, 128.1, 128.3, 136.3, 141.3, 147.6, 160.1.

Synthesis of ***4***. A solution of *N,N′*-dicyclohexylcarbodiimide (DCC; 58 mg, 0.3 mmol) in CH_2Cl_2 (5 mL) was added dropwise over the course of 10 min to a solution of **2** (100 mg, 0.2 mmol), *N*-hydroxysuccinimide (33 mg, 0.3 mmol), and 4-(dimethylamino)pyridine (DMAP; 3 mg, 0.02 mmol) in CH_2Cl_2 (15 mL) maintained at 0 °C under Ar. The reaction mixture was allowed to warm to ambient temperature and was stirred for 15 h under these conditions. The precipitate was filtered off, and *n*-decylamine (45 mg, 0.3 mmol) was added dropwise to the filtrate over the course of 10 min. The resulting solution was stirred at ambient temperature for 12 h. The precipitate was filtered off, and the solvent was distilled off under reduced pressure. The residue was purified by column chromatography [SiO_2:$CHCl_3$/MeOH (98:2, v/v)] to afford **4** (63 mg, 47%) as a red solid. FABMS: m/z = 563 $[M + H]^+$. ^1H NMR ($CDCl_3$): δ = 0.89 (3H, t, 13 Hz), 0.98 (6H, t, 15 Hz), 1.13−1.41 (14H, m), 1.25 (6H, s), 1.65−1.68 (2H, m), 2.27−2.32 (4H, m), 2.54 (6H, s), 3.49 (2H, m), 6.41 (1H, br s), 7.37 (2H, d, 8 Hz), 7.90 (2H, d, 8 Hz). ^{13}C NMR ($CDCl_3$): δ = 12.3, 12.9, 14.5, 14.9, 17.5, 23.1, 27.5, 29.7, 29.8, 29.9, 30.1, 32.3, 40.7, 128, 129.1, 130.8, 133.4, 135.5, 138.6, 139.2, 139.5, 154.6, 167.

Synthesis of ***5***. A solution of DCC (2.3 g, 11 mmol) in CH_2Cl_2 (20 mL) was added dropwise, over the course of 20 min, to a solution of 1-decanol (1.5 g, 10 mmol), DMAP (232 mg, 2 mmol), and methacrylic acid (816 mg, 10 mmol) in CH_2Cl_2 (60 mL) maintained at 0 °C under Ar. The reaction mixture was allowed to warm to ambient temperature and was stirred for 24 h under these conditions. The resulting precipitate was filtered off, and the solvent was distilled off under reduced pressure. The residue was purified by column chromatography [SiO_2:hexane/EtOAc (2:1, v/v)] to afford **5** (1.5 g, 70%) as a colorless oil. FABMS: m/z=228 $[M + H]^+$. ^1H NMR ($CDCl_3$): δ = 0.90 (3H, t, 13 Hz), 1.20−1.36 (14H, m), 1.63−1.70 (2H, m), 1.95 (3H, s), 4.15 (2H, t, 13 Hz), 5.54 (1H, s), 6.09 (1H, s). ^{13}C NMR ($CDCl_3$): δ = 14.5, 18.7, 23.1, 26.4, 29, 29.6, 29.7, 29.9, 32.3, 65.2, 125.5, 136.9, 167.9.

Synthesis of ***6***. A solution of DCC (1.2 g, 3.6 mmol) in CH_2Cl_2 (20 mL) was added dropwise, over the course of 20 min, to a solution of poly(ethylene glycol) monomethyl ether (M_n = 2000, 10 g, 5 mmol), DMAP (244 mg, 2 mmol), and methacrylic acid (860 mg, 10 mmol) in CH_2Cl_2 (80 mL) maintained at 0 °C under Ar. The reaction mixture was allowed to warm to ambient temperature and was stirred for 24 h under these conditions. The resulting precipitate was filtered off, and the solvent was distilled off under reduced pressure. The residue was purified by column chromatography [SiO_2:$CHCl_3$/MeOH (19:1, v/v)] to afford **6** (6 g, 60%) as a white solid. ^1H NMR ($CDCl_3$): δ = 1.95 (3H, s), 3.38 (3H, s), 3.54−3.88 (180H, m), 4.30 (2H, t, 5.32, 10 Hz), 5.57 (1H, s), 6.13 (1H, s).

Synthesis of ***7***. A solution of **5** (73 mg, 0.3 mmol), **6** (1 g, 0.5 mmol), and AIBN (3 mg, 0.03 mmol) in degassed THF (8 mL) was heated for 72 h at 75 °C under Ar in a sealed vial. After the solution was cooled to ambient temperature, the reaction mixture was transferred to a centrifuge tube and diluted with THF to a total volume of 10 mL. Hexane was added in portions of 1 mL, and the tube was shaken vigorously after each addition until the formation of a precipitate was clearly observed. After centrifugation, the oily layer at the bottom of the tube was separated from the supernatant and dissolved in THF (10 mL). Hexane was added in portions of 1 mL, and the tube was shaken vigorously after each addition until the formation of a precipitate was clearly observed. After centrifugation, the oily residue was separated from the supernatant and dried under reduced pressure to give **7** (0.8 g) as a white solid. GPC: M_n = 46 800, PDI = 1.73. ^1H NMR ($CDCl_3$): δ = 0.70−0.89 (3H, br s), 1.14−1.28 (8H, br s), 1.61−1.68 (2H, m), 1.95−2.07 (3H, br s), 3.38 (2H, s), 3.54−3.90 (135H, m), 4.25−4.30 (3H, br s).

Polymer Micelles. A solution of **7** (2.5 mg mL^{-1}, 100 μL) in $CHCl_3$ was added to a solution of **1a** (0.1 mg mL^{-1}, 100 μL), **2a** (0.1 mg mL^{-1}, 40 μL), **3** (0.1 mg mL^{-1}, 12 μL), or **4** (0.1 mg mL^{-1}, 30 μL) in $CHCl_3$. Alternatively, a solution of **7** (2.5 mg mL^{-1}, 200 μL) in $CHCl_3$ was mixed with solutions of **2a** (0.1 mg mL^{-1}, 20 μL) and **4** (0.1 mg mL^{-1}, 100 μL) in $CHCl_3$. Each mixture was heated at 40 °C in an open vial. After the evaporation of the solvent, the residue was purged with air and dispersed in PBS (1 mL, pH 7.4). After vigorous shaking, the dispersion was filtered, and the filtrate was used for the spectroscopic and imaging experiments without further purification.

Phospholipid Micelles. A solution of 1,2-dipalmitoyl-*sn*-glycero-3-phosphoethanolamine *N*-(methoxy(polyethylene glycol)-2000) ammonium salt (20 mg mL^{-1}, 100 μL) in $CHCl_3$ was added to a solution of **2a** (1.2 mg mL^{-1}, 33 μL) or **4** (0.6 mg mL^{-1}, 33 μL) in $CHCl_3$ maintained

at ambient temperature in an open vial. After the evaporation of the solvent, the residue was dried under reduced pressure, dispersed in H_2O (1.2 mL), heated to 80 °C for 30 s, and passed through a syringe filter (0.2 μm). Aliquots of the filtrate (100 μL) were diluted with H_2O (300 μL) and used for the spectroscopic experiments without further purification.

Intracellular Fluorescence Modulation. CHO cells were cultured in Hams-F12 essential media, supplemented with fetal bovine serum (10%, v/v), penicillin (200 U mL^{-1}), streptomycin (200 μg mL^{-1}), and glutamine (2 mM), and incubated overnight at 37 °C in O_2/CO_2/air (20:5:75, v/v/v). The cultured cells were incubated further with PBS dispersions (10%, v/v) of **4** and **7** with and without **2a** for 24 h on glass coverslips. After being washed three times with PBS (1 mL), the coverslips were imaged with an inverted Leica SP5 confocal/multiphoton microscope. The samples were excited at 514 nm, and the emission was recorded from 535 to 635 nm. Alternatively, the coverslips were transferred in well plates, and their fluorescence was measured with a Flex station luminescent plate reader. The samples were excited at 434 nm, and the emission was measured at 550 nm from the bottom of the plate with the automatic emission cut-off switched off. Ultraviolet irradiation was performed with a UVP UVGL-58 lamp, operating at 365 nm (0.4 mW cm^{-2}).

Cytotoxicity Assays. CHO cells were seeded in well plates at a density of 5×10^4 cells mL^{-1}, incubated overnight at 37 °C in O_2/CO_2/air (20:5:75, v/v/v), and spiked with increasing volumes (0−25%, v/v) of a stock PBS dispersion of **2a** (0.02 mg mL^{-1}), **4** (0.01 mg mL^{-1}), and **7** (0.25 mg mL^{-1}). The cells were incubated for a further 24 h, harvested by trypsinization, and resuspended in Hams-F12 media and Trypan Blue (0.4%, v/v). After incubation at ambient temperature for 1 min, the cells were counted with an Invitrogen Countess hemocytometer, and their viability was determined. Ultraviolet irradiation was performed with a UVP UVGL-58 lamp, operating at 365 nm (0.4 mW cm^{-2}).

■ ASSOCIATED CONTENT

Supporting Information. TEM images of polymer micelles without and with **2a** and **4** in their interior, synthesis of **2a**, absorption spectra of **2a** in MeCN, absorption spectra of **4** in MeCN and MeCN/H_2O, absorption spectra of **4** in phospholipid micelles, absorption spectra and absorbance evolution after irradiation of **2a** in phospholipid micelles, absorbance evolution after irradiation of **2a** and **4** in polymer micelles, vertical stack of fluorescence images of CHO cells incubated with **2a**, **4**, and **7**, profiles of the emission intensity measured across CHO cells incubated with **2a**, **4**, and **7**, profiles of the emission intensity measured across CHO cells incubated with **4** and **7**, relative emission intensity measured across CHO cells incubated with and without **2a**, and cytotoxicity assays. This material is available free of charge via the Internet at http://pubs.acs.org.

■ AUTHOR INFORMATION

Corresponding Author

J.Callan@ulster.ac.uk; fraymo@miami.edu

■ ACKNOWLEDGMENT

We thank the National Science Foundation (CAREER Award CHE-0237578 and CHE-0749840) and the University of Miami for financial support.

■ REFERENCES

(1) Dorion, G. H.; Wiebe, A. F. *Photochromism*; Focal Press: New York, 1970.

(2) Brown, G. H., Ed. *Photochromism*; Wiley: New York, 1971.

(3) El'tsov, A. V., Ed. *Organic Photochromes*; Consultants Bureau: New York, 1990.

(4) Bouas-Laurent, H., Dürr, H., Eds. *Photochromism: Molecules and Systems*; Elsevier: Amsterdam, 1990.

(5) Crano, J. C., Guglielmetti, R., Eds. *Organic Photochromic and Thermochromic Compounds*; Plenum Press: New York, 1999.

(6) *Photochromism: Memories and Switches*; Irie, M., Ed. *Chem. Rev.* **2000**, *100*, 1683−1890.

(7) Kuz'min, M. G.; Koz'menko, M. V. In *Organic Photochromes*; El'tsov, A. V., Ed.; Consultants Bureau: New York, 1990; pp 245−265.

(8) (a) Raymo, F. M.; Tomasulo, M. *Chem. Soc. Rev.* **2005,** *34*, 327–336. (b) Raymo, F. M.; Tomasulo, M. *J. Phys. Chem. A* **2005,** *109*, 7343–7352. (c) Cusido, J.; Deniz, E.; Raymo, F. M. *Eur. J. Org. Chem.* **2009,** 2031–2045. (d) Yildiz, I.; Deniz, E.; Raymo, F. M. *Chem. Soc. Rev.* **2009,** *38*, 1859–1867.

(9) (a) Walz, J.; Ulrich, K.; Port, H.; Wolf, H. C.; Wonner, J.; Effenberg, F. *Chem. Phys. Lett.* **1993,** *213*, 321–324. (b) Seibold, M.; Port, H.; Wolf, H. C. *Mol. Cryst. Liq. Cryst.* **1996,** *283*, 75–80. (c) Port, H.; Hennrich, M.; Seibold, M.; Wolf, H. C. *Proc.—Electrochem. Soc.* **1998,** *98*, 61–70. (d) Port, H.; Hartschuh, A.; Hennrich, M.; Wolf, H. C.; Endtner, J. M.; Effenberger, F. *Mol. Cryst. Liq. Cryst.* **2000,** *344*, 145–150. (e) Ramsteiner, I. B.; Hartschuh, A.; Port, H. *Chem. Phys. Lett.* **2001,** *343*, 83–90.

(10) (a) Norsten, T. B.; Branda, N. R. *Adv. Mater.* **2001,** *13*, 347–349. (b) Myles, A. J.; Branda, N. R. *J. Am. Chem. Soc.* **2001,** *123*, 177–178. (c) Norsten, T. B.; Branda, N. R. *J. Am. Chem. Soc.* **2001,** *123*, 1784–1785. (d) Myles, A.; Branda, N. R. *Adv. Funct. Mater.* **2002,** *12*, 167–173.

(11) (a) Kawai, T.; Sasaki, T.; Irie, M. *Chem. Commun* **2001,** 711–712. (b) Giordano, L.; Jovin, T. M.; Irie, M.; Jares-Erijman, E. A. *J. Am. Chem. Soc.* **2002,** *124*, 7481–7489. (c) Irie, M.; Fukaminato, T.; Sasaki, T.; Tamai, N.; Kawai, T. *Nature* **2002,** *420*, 759–760. (d) Kim, M.-S.; Kawai, T.; Irie, M. *Opt. Mater.* **2002,** 275–278. (e) Fukaminato, T.; Sasaki, T.; Kawai, T.; Tamai, N.; Irie, M. *J. Am. Chem. Soc.* **2004,** *126*, 14843–14849. (f) Jares-Erijman, E. A.; Giordano, L.; Spagnuolo, C.; Kawior, J.; Verneij, R. J.; Jovin, T. M. *Proc. SPIE—Int. Soc. Opt. Eng.* **2004,** *5323*, 13–26.

(12) (a) Bahr, J. L.; Kodis, G.; de la Garza, L.; Lin, S.; Moore, A. L.; Moore, T. A.; Gust, D. *J. Am. Chem. Soc.* **2001,** *123*, 7124–7133. (b) Andréasson, J.; Kodis, G.; Terazono, Y.; Liddell, P. A.; Bandyopadhyay, S.; Mitchell, R. H.; Moore, T. A.; Moore, A. L.; Gust, D. *J. Am. Chem. Soc.* **2004,** *126*, 15926–15927. (c) Terazono, Y.; Kodis, G.; Andréasson, J.; Jeong, G.; Brune, A.; Hartmann, T.; Dürr, H.; Moore, T. A.; Moore, A. L.; Gust, D. *J. Phys. Chem. B* **2004,** *108*, 1812–1814. (d) Straight, S. D.; Andréasson, J.; Kodis, G.; Bandyopadhyay, S.; Mitchell, R. H.; Moore, T. A.; Moore, A. L.; Gust, D. *J. Am. Chem. Soc.* **2005,** *127*, 9403–9409. (e) Straight, S. D.; Liddell, P. A.; Terazono, Y.; Moore, T. A.; Moore, A. L.; Gust, D. *Adv. Funct. Mater.* **2007,** *17*, 777–785.

(13) (a) Tomasulo, M.; Deniz, E.; Alvarado, R. J.; Raymo, F. M. *J. Phys. Chem. C* **2008,** *112*, 8038–8045. (b) Deniz, E.; Sortino, S.; Raymo, F. M. *J. Phys. Chem. Lett.* **2010,** *1*, 1690–1693. (c) Deniz, E.; Tomasulo, M.; DeFazio, R. A.; Watson, B. D.; Raymo, F. M. *Phys. Chem. Chem. Phys.* **2010,** *12*, 11630–11634. (d) Deniz, E.; Ray, S.; Tomasulo, M.; Impellizzeri, S.; Sortino, S.; Raymo, F. M. *J. Phys. Chem. A* **2010,** *114*, 11567–11575.

(14) (a) Medintz, I. L.; Trammell, S. A.; Mattoussi, H.; Mauro, J. M. *J. Am. Chem. Soc.* **2004,** *126*, 30–31. (b) Medintz, I. L.; Clapp, A. R.; Trammell, S. A.; Mattoussi, H. *Proc. SPIE—Int. Soc. Opt. Eng.* **2004,** *5593*, 300–307.

(15) (a) Harbron, E. J.; Vicente, D. A.; Hoyt, M. T. *J. Phys. Chem. B* **2004,** *108*, 18789–18792. (b) Harbron, E. J.; Vicente, D. A.; Hadley, D. H.; Imm, M. R. *J. Phys. Chem. A* **2005,** *109*, 10846–10853. (c) Grimes, A. F.; Call, S. E.; Vicente, D. A.; English, D. S.; Harbron, E. J. *J. Phys. Chem. B* **2006,** *110*, 19183–19190. (d) Lewis, S. M.; Harbron, E. J. *J. Phys. Chem. C* **2007,** *111*, 4425–4430.

(16) (a) Zhu, L.; Zhu, M.-Q.; Hurst, J. K.; Li, A. D. Q. *J. Am. Chem. Soc.* **2005,** *127*, 8968–8970. (b) Zhu, M.-Q.; Zhu, L.; Han, J. J.; Wu, W.; Hurst, J. K.; Li, A. D. Q. *J. Am. Chem. Soc.* **2006,** *128*, 4303–4309.

(c) Zhu, L.; Wu, W.; Zhu, M.-Q.; Han, J. J.; Hurst, J. K.; Li, A. D. Q. *J. Am. Chem. Soc.* **2007,** *129,* 3524–3526. (d) Hu, D.; Tian, Z.; Wu, W.; Wan, W.; Li, A. D. Q. *J. Am. Chem. Soc.* **2008,** *130,* 15279–15281.

(17) (a) Jares-Erijman, E.; Giordano, L.; Spagnuolo, C.; Lidke, K. A.; Jovin, T. M. *Mol. Cryst. Liq. Cryst.* **2005,** *430,* 257–265. (b) Mikoski, S.; Giordano, L.; Etchelon, M. H.; Menendez, G.; Lidke, K. A.; Hagen, G. M.; Jovin, T. M.; Jares-Erijman, E. *Proc. SPIE—Int. Soc. Opt. Eng.* **2006,** *6096,* 60960X–1−60960X-8.

(18) Finden, J.; Kunz, T. K.; Branda, N. R.; Wolf, M. O. *Adv. Mater.* **2008,** *20,* 1998–2002.

(19) (a) Hofmann, M.; Eggeling, C.; Jakobs, S.; Hell, S. W. *Proc. Natl. Acad. Sci. U.S.A.* **2005,** *102,* 17565–17569. (b) Bossi, M.; Belov, V.; Polyakova, S.; Hell, S. W. *Angew. Chem., Int. Ed.* **2006,** *45,* 7462–7465. (c) Bossi, M.; Fölling, J.; Dyba, M.; Westphal, V.; Hell, S. W. *New J. Phys.* **2006,** *8,* 275–284. (d) Schwentker, M. A.; Bock, H.; Hofmann, M.; Jakobs, S.; Bewersdorf, J.; Eggeling, C.; Hell, S. W. *Microsc. Res. Tech.* **2007,** *70,* 269–280. (e) Fölling, J.; Polyakova, S.; Belov, V.; van Blaaderen, A.; Bossi, M. L.; Hell, S. W. *Small* **2008,** *4,* 134–142.

(20) (a) Hell, S. W. *Nat. Biotechnol.* **2003,** *21,* 1347–1355. (b) Hell, S. W.; Dyba, M.; Jakobs, S. *Curr. Opin. Neurobiol.* **2004,** *14,* 599–609. (c) Hell, S. W. *Phys. Lett. A* **2004,** *326,* 140–145. (d) Hell, S. W.; Kastrup, L. *Nachr. Chem.* **2007,** *55,* 47–50. (e) Hell, S. W. *Science* **2007,** *316,* 1153–1158. (f) Hell, S. W. *Nat. Methods* **2009,** *6,* 24–32. (g) Hell, S. W.; Schmidt, R.; Egner, A. *Nat. Photonics* **2009,** *3,* 381–387.

(21) (a) Bates, M.; Huang, B.; Zhuang, X. *Curr. Opin. Chem. Biol.* **2008,** *12,* 505–514. (b) Huang, B.; Bates, M.; Zhuang, X. *Annu. Rev. Biochem.* **2009,** *78,* 993–1016. (c) Zhuang, X. *Nat. Photonics* **2009,** *3,* 365–367. (d) Huang, B. *Curr. Opin. Chem. Biol.* **2010,** *14,* 10–14.

(22) Ji, N.; Shroff, H.; Zhong, H.; Betzig, E. *Curr. Opin. Neurobiol.* **2008,** *18,* 605–616.

(23) Gustafsson, M. G. L. *Nat. Methods* **2008,** *5,* 385–387.

(24) Fernández-Suárez, M.; Ting, A. Y. *Nat. Rev. Mol. Cell. Biol.* **2008,** *9,* 929–943.

(25) Heilemann, M.; Dedecker, P.; Hofkens, J.; Sauer, M. *Laser Photon Rev.* **2009,** *3,* 180–202.

(26) (a) Lippincott-Schwartz, J.; Manley, S. *Nat. Methods* **2009,** *6,* 21–23. (b) Lippincott-Schwartz, J.; Patterson, G. H. *Trends Cell Biol.* **2009,** *19,* 555–565. (c) Manley, S.; Gillette, J. M.; Lippincott-Schwartz, J. *Methods Enzymol.* **2010,** *475,* 109–120.

(27) Hess, S. T. *Nat. Methods* **2009,** *6,* 124–125.

(28) Vogelsang, J.; Steinhauer, C.; Forthmann, C.; Stein, I. H.; Person-Skergo, B.; Cordes, T.; Tinnefeld, P. *ChemPhysChem* **2010,** *11,* 2475–2490.

(29) Wessels, J. T.; Yamauchi, K.; Hoffman, R. M.; Wouters, F. S. *Cytometry* **2010,** *77A,* 667–676.

(30) Toprak, E.; Kural, C.; Selvin, P. R. *Methods Enzymol.* **2010,** *475,* 1–26.

(31) Thompson, M. A.; Biteen, J. S.; Lord, S. J.; Conley, N.; Moerner, W. E. *Methods Enzymol.* **2010,** *475,* 27–59.

(32) Cusido, J.; Impellizzeri, S.; Raymo, F. M. *Nanoscale* **2010,** 10.1039/c0nr00546k.

(33) (a) Allen, C.; Maysinger, D.; Eisenberg, A. *Colloids Surf., B* **1999,** *16,* 3–27. (b) Savić, R.; Eisenberg, A.; Maysinger, D. *J. Drug Targeting* **2006,** *14,* 343–355.

(34) Jones, M.-C.; Leroux, J.-C. *Eur. J. Pharm. Biopharm.* **1999,** *48,* 101–111.

(35) Moghimi, S. M.; Hunter, A. C.; Murray, J. C. *Pharmacol. Rev.* **2001,** *53,* 283–316.

(36) (a) Torchilin, V. P. *Cell. Mol. Life Sci.* **2004,** *61,* 2459–2559. (b) Torchilin, V. P. *Pharm. Res.* **2007,** *27,* 1–16.

(37) Rapoport, N. *Prog. Polym. Sci.* **2007,** *32,* 962–990.

(38) (a) Raymo, F. M.; Giordani, S. *J. Am. Chem. Soc.* **2001,** *123,* 4651–4652. (b) Raymo, F. M.; Giordani, S.; White, A. J. P.; Williams, D. J. *J. Org. Chem.* **2003,** *68,* 4158–4169.

(39) For examples of similar amphiphilic polymers, see: (a) Aathimanikandan, S. V.; Savariar, E. N.; Thayumanavan, S. *J. Am. Chem. Soc.* **2005,** *127,* 14922–14929. (b) Ryu, J.-H.; Roy, R.; Ventura, J.; Thayumanavan, S. *Langmuir* **2010,** *26,* 7086–7092.

(40) Maa, Y. F.; Chen, S. H. *Macromolecules* **1988,** *21,* 1176–1177.

(41) Tomasulo, M.; Giordani, S.; Raymo, F. M. *Adv. Funct. Mater.* **2005,** *15,* 787–794.

(42) Dubertret, B.; Skourides, P.; Norris, D. J.; Noireaux, V.; Brivanlou, A. H.; Libchaber, A. *Science* **2002,** *298,* 1759–1762.

(43) (a) Zhang, L. W.; Yu, W. W.; Colvin, V. L.; Monteiro-Riviere, N. A. *Toxicol. Appl. Pharmacol.* **2008,** *228,* 200–211. (b) Zhang, L. W.; Monteiro-Riviere, N. A. *Toxicol. Sci.* **2009,** *110,* 138–155−211.

(44) (a) Yildiz, I.; McCaughan, B.; Cruickshank, S. F.; Callan, J. F.; Raymo, F. M. *Langmuir* **2009,** *25,* 7090–7096. (b) Yildiz, I.; Deniz, E.; McCaughan, B.; Cruickshank, S. F.; Callan, J. F.; Raymo, F. M. *Langmuir* **2010,** *26,* 11503–11511.

(45) Freshney, R. I. *Culture of Animal Cells—A Manual of Basic Techniques*; Wiley: New York, 2005.

(46) Lakowicz, J. R. *Principles of Fluorescence Spectroscopy*; Springer: New York, 2006.